DAFTAR PUSTAKA

[1] T. Ayode Otitoju, P. Ugochukwu Okoye, G. Chen, Y. Li, M. Onyeka Okoye, and S. Li, "Advanced ceramic components: Materials, fabrication, and applications," J. Ind. Eng. Chem., vol. 85, pp. 34–65, 2020, doi: 10.1016/j.jiec.2020.02.002.

[2] Benzerga, R., Laur, V., Lebullenger, R., Gendre, L. L., Genty, S., Sharaiha, A., & Queffelec, P. (2015). Waste-glass recycling: A step toward microwave applications. Materials Research Bulletin, 67, 261–265. doi:10.1016/j.materresbull.2014.07.037

[3] Y. Liu, H. Lv, X. Lan, J. Leng, and S. Du, "Review of electro-active shape-memory polymer composite," Compos. Sci. Technol., vol. 69, no. 13, pp. 2064–2068, 2009, doi: 10.1016/j.compscitech.2008.08.016.

[4] Jusoh, W. N. W., Matori, K. A., Zaid, M. H. M., Zainuddin, N., Khiri, M. Z. A., Rahman, N. A. A., Kul, E. (2019). Effect of sintering temperature on physical and structural properties of Alumino-Silicate-Fluoride glass ceramics fabricated from clam shell and soda lime silicate glass. Results in Physics, 12, 1909–1914. doi:10.1016/j.rinp.2019.01.077

[5] Hisham, N. A. N., Zaid, M. H. M., Saparuddin, D. I., Aziz, S. H. A., Muhammad, F. D., Honda, S., & Iwamoto, Y. (2020). Crystal growth and mechanical properties of porous glass-ceramics derived from waste soda-lime-silica glass and clam shells. Journal of Materials Research and Technology, 9(4), 9295–9298. doi:10.1016/j.jmrt.2020.06.009

[6] Tang, Y.-L., Yin, H.-L., Zhao, Q., Liu, H., Sun, X.-X., Huang, M.-Q., Pan, J.-W. (2016). Measurement-Device-Independent Quantum Key Distribution over Untrustful Metropolitan Network. Physical Review X, 6(1). doi:10.1103/physrevx.6.011024

[7] A. Panigrahi, H. Jena, and B. Surekha, "Effect of Clams Shell in Impact Properties of Jute Epoxy Composite," Mater. Today Proc., vol. 5, no. 9, pp. 19997–20001, 2018, doi: 10.1016/j.matpr.2018.06.366.

[8] S. Baumgartner, R. Gmeiner, J. A. Schönherr, and J. Stampfl,

"Stereolithography-based additive manufacturing of lithium disilicate glass ceramic for dental applications," Mater. Sci. Eng. C, vol. 116, no. December 2019, p. 111180, 2020, doi: 10.1016/j.msec.2020.111180.

[9] S. S. Liu, M. Li, J. M. Wu, A. N. Chen, Y. S. Shi, and C. H. Li, "Preparation of high-porosity Al_2O_3 ceramic foams via selective laser sintering of Al2O3 poly-hollow microspheres," Ceram. Int., vol. 46, no. 4, pp. 4240–4247, 2020, doi: 10.1016/j.ceramint.2019.10.144.

[10] Fabris, D. C. N., Polla, M. B., Acordi, J., Luza, A. L., Bernardin, A. M., De Noni, A., & Montedo, O. R. K. (2020). Effect of MgO·Al2O3·SiO2 glass-ceramic as sintering aid on properties of alumina armors. Materials Science and Engineering: A, 781, 139237. doi:10.1016/j.msea.2020.139237

[11] M. Olivia, A. A. Mifshella, and L. Darmayanti, "Mechanical properties of seashell concrete," Procedia Eng., vol. 125, pp. 760–764, 2015, doi: 10.1016/j.proeng.2015.11.127.

[12] G. Li, X. Xu, E. Chen, J. Fan, and G. Xiong, "Properties of cement-based bricks with oyster-shells ash," J. Clean. Prod., vol. 91, pp. 279–287, 2015, doi: 10.1016/j.jclepro.2014.12.023.

[13] E. I. Yang, M. Y. Kim, H. G. Park, and S. T. Yi, "Effect of partial replacement of sand with dry oyster shell on the long-term performance of concrete," Constr. Build. Mater., vol. 24, no. 5, pp. 758–765, 2010, doi: 10.1016/j.conbuildmat.2009.10.032.

[14] C. Martínez-García, B. González-Fonteboa, F. Martínez-Abella, and D. Carro- López, "Performance of mussel shell as aggregate in plain concrete," Constr. Build. Mater., vol. 139, pp. 570–583, 2017, doi: 10.1016/j.conbuildmat.2016.09.091.

[15] K. H. Mo, U. J. Alengaram, M. Z. Jumaat, S. P. Yap, and S. C. Lee, "Green concrete partially comprised of farming waste residues: A review,"J. Clean. Prod., vol. 117, pp. 122–138, 2016, doi: 10.1016/j.jclepro.2016.01.022.

[16] E. Bernardo and F. Albertini, "Glass foams from dismantled cathode ray tubes,"Ceram. Int., vol. 32, no. 6, pp. 603–608, 2006, doi: 10.1016/j.ceramint.2005.04.019.

[17] P. K. Rao, P. Jana, M. I. Ahmad, and P. K. Roy, “Synthesis and characterization of zirconia toughened alumina ceramics prepared by co-precipitation method,” Ceram. Int., vol. 45, no. 13, pp. 16054–16061, 2019, doi: 10.1016/j.ceramint.2019.05.121.

[18] Y. Shahmoradi, D. Souri, and M. Khorshidi, “Glass-ceramic nanoparticles in the Ag2O–TeO2–V2O5 system: Antibacterial and bactericidal potential, their structural and extended XRD analysis by using Williamson–Smallman approach,” Ceram. Int., vol. 45, no. 5, pp. 6459–6466, 2019, doi: 10.1016/j.ceramint.2018.12.133.

[19] Khiri, M. Z. A., Matori, K. A., Zaid, M. H. M., Abdullah, A. C., Zainuddin, N., Jusoh, W. N. W., Effendy, N. (2020). Soda lime silicate glass and clam Shell act as precursor in synthesize calcium fluoroaluminosilicate glass to fabricate glass ionomer cement with different ageing time. Journal of Materials Research and Technology, 9(3), 6125–6134. doi:10.1016/j.jmrt.2020.04.015

[20] S. C. Wu, H. C. Hsu, S. K. Hsu, C. P. Tseng, and W. F. Ho, “Effects of calcination on synthesis of hydroxyapatite derived from oyster shell powders,” J. Aust. Ceram. Soc., vol. 55, no. 4, pp. 1051–1058, 2019, doi: 10.1007/s41779-019-00317-7.

[21] Khiri, M. Z. A., Matori, K. A., Zaid, M. H. M., Abdullah, C. A. C., Zainuddin, N., Alibe, I. M., Effendy, N. (2019). Crystallization behavior of low-cost biphasic hydroxyapatite/β-tricalcium phosphate ceramic at high sintering temperatures derived from high potential calcium waste sources. Results in Physics, 12, 638–644. doi:10.1016/j.rinp.2018.12.025

[22] S. C. Wu, H. C. Hsu, S. K. Hsu, C. P. Tseng, and W. F. Ho, “Preparation and characterization of hydroxyapatite synthesized from oyster shell powders,” Adv. Powder Technol., vol. 28, no. 4, pp. 1154–1158, 2017, doi: 10.1016/j.apt.2017.02.001.

[23] S. Hussain and K. Sabiruddin, “Effect of heat treatment on the synthesis of hydroxyapatite from Indian clam seashell by hydrothermal method,” Ceram. Int., vol. 47, no. 21, pp. 29660–29669, 2021.

[24] Rahman, N. A. A., Matori, K. A., Zaid, M. H. M., Zainuddin, N., Aziz, S. A., Khiri, M. Z. A., Jusoh, W. N. W. (2019). Fabrication of Alumino-Silicate-Fluoride based bioglass derived from waste clam shell and soda lime silica glasses. Results in Physics, 12, 743–747.

[25] A. Sobczak-Kupiec, K. Pluta, A. Drabczyk, M. Włoś, and B. Tyliszczak, "Synthesis and characterization of ceramic - polymer composites containing bioactive synthetic hydroxyapatite for biomedical applications," Ceram. Int., vol. 44, no. 12, pp. 13630–13638, 2018.

[26] Chen, A.-N., Li, M., Xu, J., Lou, C.-H., Wu, J.-M., Cheng, L.-J., Li, C.-H. (2018). High-porosity mullite ceramic foams prepared by selective laser sintering using fly ash hollow spheres as raw materials. Journal of the European Ceramic Society, 38(13), 4553–4559.

[27] Ru, Jianhong; Fan, Yuchi; Zhou, Weiwei; Zhou, Zhenxing; Wang, Tuo; Liu, Ruiheng; Yang, Jianping; Lu, Xiaofang; Wang, Jiancheng; Ji, Chengchang; Wang, Lianjun; Jiang, Wan (2018). Electrically conductive and mechanically strong graphene/mullite ceramic composites for high-performance electromagnetic interference shielding. ACS Applied Materials & Interfaces, acsami.8b12933–. doi:10.1021/acsami.8b12933

[28] E. Barrachina, M. Esquinas, J. Llop, M. D. Notari, and J. B. Carda, "Development of a glass-ceramic glaze formulated from industrial residues to improve the mechanical properties of the porcelain stoneware tiles," Mater. Lett., vol. 220, pp. 226–228, 2018, doi: 10.1016/j.matlet.2018.03.023.

[29] A. M. Abdelghany, I. M. Elkashef, and H. A. ElBatal, "Manifestation and Role of B_2O_3 in High Lead Containing Silicate Glasses," Silicon, vol. 10, no. 3, pp. 1103–1110, 2018, doi: 10.1007/s12633-017-9577-2.

[30] A. M. Abdelghany, H. M. Zeyada, H. A. ElBatal, and R. Fetouh, "Synthesis and Spectral Properties of Nd2O3-Doped Sodium Silicophosphate Glass," Silicon, vol. 8, no. 2, pp. 325–330, 2016, doi: 10.1007/s12633-015-9308-5.

[31] P. Budhathoki, G. Paudyal, R. Oli, N. Duwal, and J. Bhattarai, "Assessment on the Characterization of Mineralogical Phase of Ceramic Tiles Available

in Kathmandu Valley (Nepal) Using XRD and FTIR Analyses," Int. J. Appl. Sci. Biotechnol., vol. 6, no. 3, pp. 238–243, 2018, doi: 10.3126/ijasbt.v6i3.21171.

[32] H. Kaur, V. K. Bulasara, and R. K. Gupta, "Influence of pH and temperature of dip-coating solution on the properties of cellulose acetate-ceramic composite membrane for ultrafiltration," Carbohydr. Polym., vol. 195, pp. 613–621, 2018, doi: 10.1016/j.carbpol.2018.04.121.

[33] Chen, X., Gao, X., Fu, K., Qiu, M., Xiong, F., Ding, D., Drioli, E. (2018). Tubular hydrophobic ceramic membrane with asymmetric structure for water desalination via vacuum membrane distillation process. Desalination, 443, 212–220. doi:10.1016/j.desal.2018.05.027

[34] M. H. M. Zaid, K. A. Matori, S. H. A. Aziz, Z. A. Wahab, and S. S. A. Rashid, "Effect of sintering on crystallization and structural properties of soda lime silica glass," Sci. Sinter., vol. 49, no. 4, pp. 409–417, 2017, doi: 10.2298/SOS1704409Z.

[35] F. Rouabhia, A. Nemamcha, and H. Moumeni, "Elaboration and characterization of mullite-anorthite-albite porous ceramics prepared from Algerian kaolin," Ceramica, vol. 64, no. 369, pp. 126–132, 2018, doi: 10.1590/0366-69132018643692297.

[36] H. Mohamad, P. Yan, N. F. Ibrahim, and S. N. F. M. Noor, "Effects of alumina (Al_2O_3) addition on mechanical property of fabricated melt-derived bioactive glass," AIP Conf. Proc., vol. 1791, 2016, doi: 10.1063/1.4968878.

[37] N. H. A. S. Lim, H. Mohammadhosseini, M. M. Tahir, M. Samadi, and A. R. M. Sam, "Microstructure and Strength Properties of Mortar Containing Waste Ceramic Nanoparticles," Arab. J. Sci. Eng., vol. 43, no. 10, pp. 5305–5313, 2018, doi: 10.1007/s13369-018-3154-x.

[38] K. T. Stanton, K. P. O'Flynn, S. Kiernan, J. Menuge, and R. Hill, "Spherulitic crystallization of apatite-mullite glass-ceramics: Mechanisms of formation and implications for fracture properties," J. Non. Cryst.

Solids, vol. 356, no. 35–36, pp. 1802–1813, 2010, doi: 10.1016/j.jnoncrysol.2010.07.006.

[39] L. Pérez-Villarejo, F. Takabait, L. Mahtout, B. Carrasco-Hurtado, D. Eliche-Quesada, and P. J. Sánchez-Soto, "Synthesis of vaterite $CaCO_3$ as submicron and nanosized particles using inorganic precursors and sucrose in aqueous medium," Ceram. Int., vol. 44, no. 5, pp. 5291–5296, 2018, doi: 10.1016/j.ceramint.2017.12.142.

[40] J. König, R. R. Petersen, and Y. Yue, "Fabrication of highly insulating foam glass made from CRT panel glass," Ceram. Int., vol. 41, no. 8, pp. 9793–9800, 2015, doi: 10.1016/j.ceramint.2015.04.051.

[41] Li, Zhaohao; Zhang, Heng; Chen, Haiping; Huang, Jiguang; Fu, Hongming (2020). Water vapor capture using microporous ceramic membrane. Desalination, 482, 114405.

LAMPIRAN 1

Tabel 1.1 Unsur Komposisi Cangkang sebelum kalsinasi

Unsur-unsur	Komposisi (Wt %)
Ca	95,450
Mg	3,970
Sr	0,466
Nb	0,0254
Br	0,025
Mo	0,018
Sb	0,008
In	0,007
Ru	0,007
Te	0,007
Sn	0,007

Tabel 1.2 Unsur Komposisi Cangkang setelah kalsinasi

Unsur-unsur	Komposisi (Wt %)
Ca	99,360
Sr	0,475
Ti	0,0468
Cr	0,029
V	0,029
Nb	0,016
Mo	0,011
In	0.0051

Tabel 1.3 Unsur Komposisi Kaca

Unsur-unsur	Komposisi (Wt %)
Si	63,680
Ca	26,990
Fe	4,150
Ti	3,570
Cr	0,771
K	0,410
Zr	0,315
Sn	0,037
Nb	0,025

Y	0,022
In	0,009
Sb	0,009
Te	0,008

Tabel 1.4 Tabel Unsur Komposisi Pasir

Unsur-unsur	Komposisi (Wt %)
Si	43,670
Fe	31,000
K	9,940
Ca	6,460
Al	4,390
Ti	2,790
Mn	0,600
Sr	0,352
Px	0,251
Zr	0,229
Ba	0,107
Rb	0,072
Nb	0,041
Zn	0,039
Mo	0,025
In	0,012
Ru	0,009
Sn	0,008
Sb	0,007
Rh	0,006

LAMPIRAN 2

Tabel 2.1 Data Hasil FTIR

Bilangan gelombang (cm^{-1})	Transmitansi		
	700 ^{0}C	800 ^{0}C	900 ^{0}C
339,4716	2,23889	1,71977	80,94124
341,4004	105,319	97,33075	102,9206
343,3293	96,18857	99,3679	96,34558
345,2581	92,55144	100,9609	88,46519
347,1869	89,81854	98,00729	79,47672
349,1157	89,83798	98,45195	69,73932
351,0445	88,84447	94,11307	59,97882
352,9733	88,7878	86,32967	51,53988
354,9021	87,62234	74,61863	45,57096
356,831	99,16856	65,27208	40,06862
358,7598	96,21848	52,7702	33,45596
360,6886	95,78175	41,98369	23,01439
362,6174	91,19859	29,13706	11,82409
364,5462	92,49556	23,97009	4,12234
366,475	81,48694	21,93014	5,59147
368,4039	77,22328	22,48221	6,73218
370,3327	67,22077	20,36593	7,77504
372,2615	65,1316	21,13952	8,48473
374,1903	61,28335	20,16561	8,8494
376,1191	59,29434	19,93851	8,85086
378,0479	55,51378	18,34396	8,62904
379,9768	52,97354	17,24981	8,63042
381,9056	49,45681	15,75007	8,68708
383,8344	47,96913	15,24256	8,80856
385,7632	45,45641	14,4944	8,69538
387,692	44,57167	14,49337	8,52461
389,6208	42,55203	14,52473	8,3494
391,5497	41,71431	15,06346	8,18653
393,4785	40,1459	14,62486	8,13169
395,4073	39,28272	14,37825	8,31676
397,3361	38,07346	13,82682	8,55075
399,2649	37,63848	13,65856	8,83918
401,1937	36,88242	13,19173	9,15081
403,1225	36,98742	13,02891	9,71568

405,0514	36,6183	12,56331	10,40264
406,9802	36,72942	12,41256	11,02403
408,909	36,67726	12,16465	11,53122
410,8378	37,40591	12,31197	11,98021
412,7666	37,50959	12,45056	12,18695
414,6954	38,05204	13,0153	12,4457
416,6243	38,28157	13,33478	12,78918
418,5531	38,85736	13,70573	13,25254
420,4819	39,16462	13,88843	13,74428
422,4107	39,73562	14,22732	14,32313

LAMPIRAN 3

3.1 Data Hasil XRD

Hasil XRD pada sampel dihitung dengan persamaan sebagai berikut:

$$D = \frac{k\lambda}{B \cos \theta}$$

$$D = \frac{0,98(0,154)}{0,15\ (0,98)}$$

$$D = \frac{0,151}{0,147}$$

$$= 1,027 \text{ (nm)}$$

k = Faktor Bentuk Kristal (0,9-1)
λ = Panjang Gelombang Sinar X (0,154 nm)
R2 = 0,79523
B = Nilai Dari Full Width at Half Maximum (FWMH)
θ = Sudut Difraksi

Tabel 3.1 Data Hasil XRD

2θ (deg)	2θ (rad)	cos θ	FWHM (deg)	FWHM (rad)	D (nm)	Sin θ(Rad)
17,95947	0,313451883	0,987743608	0,60989	0,010644589	14,3540247	0,156085119
21,86991	0,381701937	0,981843167	11,55666	0,201701768	0,76207018	0,189694481
23,23907	0,405598287	0,979506635	15,24773	0,266123092	0,57897106	0,201411896
25,38927	0,443126356	0,975555125	0,91871	0,016034514	9,64804167	0,219754857
27,14895	0,473838566	0,972065659	0,71383	0,012458684	12,4617499	0,234709086
29,49518	0,514788004	0,967056647	1,15066	0,020082806	7,77088529	0,254561272
32,62355	0,569388361	0,959747591	2,34807	0,040981553	3,83708446	0,280863955
34,38319	0,600099873	0,955321731	1,11186	0,019405618	8,14084837	0,295567912

39,46671	0,688824034	0,941274144	9,6086	0,167701707	0,95607769	0,337643283
43,33809	0,756392362	0,929332198	1,08494	0,018935775	8,57615702	0,369244724
47,24852	0,824642241	0,916193133	3,20672	0,055967822	2,94321072	0,400737
50,76785	0,886066137	0,9034556	1,26936	0,022154511	7,54011216	0,428681675
57,22008	0,998678794	0,87789908	0,95315	0,016635606	10,333884	0,4788457
62,89013	1,097639836	0,853140742	0,93436	0,016307658	10,8476211	0,521680816

LAMPIRAN 4

4.1 Data Hasil Uji Densitas

Densitas pada sampel dihitung dengan persamaan sebagai berikut:

$$\rho = \frac{W_a}{W_a - W_b}\rho_b$$

dimana Wa adalah berat di udara, Wb adalah berat dalam air suling dan ρb adalah massa jenis air suling, yaitu 1,0 g/cm^3. Satuan massa jenis adalah gram per sentimeter kubik (g/cm^3).

Untuk setiap sampel dengan volume aquades sebanyak 80 ml

$$\rho = \frac{1{,}91}{81{,}80 - 80{,}00}1$$

$$\rho = 1{,}06\ (\frac{\text{gr}}{\text{cm3}})$$

Tabel 4.1 Data Hasil Densitas

Suhu (^{0}C)	Berat sampel di udara (gr)	Selisih Berat sampel di air (ml)	Massa Jenis air (1 g/cm^3)	Kerapatan (gr/cm^3)
700 (sampel I)	1,91	1,80	1,00	1,06
800 (sampel I)	2,50	2,00	1,00	1,25
900 (sampel I)	3,10	2,00	1,00	1,55
700 (sampel II)	2,76	2,00	1,00	1,38
800 (sampel II)	2,35	2,00	1,00	1,17
900 (sampel II)	3,06	2,00	1,00	1,53

LAMPIRAN 5

Alat dan Bahan Penelitian

Alat penelitian yang digunakan

z

Furnace pemanasan suhu rendah

Oven

Blender

Ball Miling

Neraca Analitik

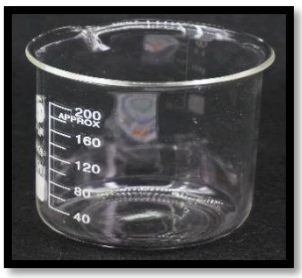

Gelas Kimia

Cawan Porselin

Ayakan 200 mesh

Furnace pemanasan suhu tinggi

Bahan Penelitian yang digunakan

Aquades

Kaca

Cangkang Kerang

Pasir Pantai

Alumina